Multiphonon absorption in ionic crystals*

L. L. Boyer, James A. Harrington†, Marvin Hass, and Herbert B. Rosenstock
U.S. Naval Research Laboratory, Washington, D.C. 20375
(Received 12 September 1974)

Calculations of the frequency and temperature dependence of infrared multiphonon absorption for the alkali halides and alkaline-earth flourides are compared with previously published data and some new results. The temperature dependence of the infrared absorption of pure crystals of NaF, NaCl, and KCl at 10.6 μm from room temperature to close to the melting point are reported. The calculations are based upon a simple approach involving and interatomic Morse-potential function in which lattice dispersion is introduced via a multiphonon frequency distribution. Good agreement between experiment and theory is obtained in which the "observed" lattice density-of-states and thermal-expansion-coefficient data (which determine the degree of anharmonicity) are the principal input to the calculations. Some structure in the multiphonon spectrum is predicted for some compounds at low temperatures, which has not yet been observed expermentally. Since the Morse potential has an exact quantum-mechanical solution, the anharmonicity is contained in the calculations without resorting to perturbation theory.

I. INTRODUCTION

The absorption of infrared radiation by ionic crystals in the "transparent" frequency region well above the reststrahl line has been of recent interest because of its application in windows for high-power infrared lasers. At these frequencies the absorption can be attributed to "intrinsic" processes involving several phonons or to defect modes involving impurities, vacancies, or surfaces. A number of theoretical approaches[1-7] have been developed to calculate the frequency and temperature dependence of the intrinsic multiphonon absorption. In this investigation a detailed set of calculations has been carried out using an extension of one of the earlier theories.[7] The results are compared with existing experimental data and some new data on specially purified crystals.

The "intrinsic" absorption may be due to two possible mechanisms: anharmonic coupling of phonons to the reststrahl mode, which is possible even in a crystal of rigid ions, though not in a wholly harmonic one ("anharmonicity"); a displacement-induced electric moment of the ions themselves, which can couple directly to the radiation ("higher-order moments"). Strictly speaking, these two mechanisms are not wholly distinct, since they both result physically from "charge overlap." Traditionally, however, theories have made this distinction. The bulk of past work on ionic crystals deals with anharmonically induced absorption with the higher-order-moments mechanism receiving attention only very recently.[2c,3,4b,4c,6c] The effect of higher-order moments is expected to be less important for the highly ionic compounds since the constituent ions are generally less polarizable. The theory developed here treats specifically only the anharmonically induced absorption, although the formalism can be adapted to handle the higher-order moments.

Two fundamentally different approaches have been taken to calculate the anharmonically induced absorption in ionic crystals. The most common approach requires the solution of the harmonic-lattice problem followed by a perturbation treatment of the anharmonicity. Sham and Sparks[2] and McGill *et al.*[3] employ diagrammatic techniques for evaluating the Green's functions, while Bendow *et al.*[4] use the equation-of-motion method. Calculations using these methods become increasingly complex for higher-order processes and consequently simplifying assumptions and approximations are made. Namjoshi and Mitra[5] take a simpler phenomenological approach in treating the perturbation. A problem with all these perturbation treatments, in addition to convergence problems and the complexities and calculational difficulties involved, is that they predict the observed temperature dependence only after "renormalization" is introduced through an *ad hoc* "temperature-dependent density of states."[8-10] Logically, the temperature dependence of the phonon spectra, just like that of the absorption coefficient, should be predicted by, rather than introduced into, the theory.

Our approach attacks the problem from the opposite point of view: Believing the anharmonicity to be of the essence in a problem that requires the interaction of many phonons, we begin with an exactly solvable anharmonic potential (Morse) and superimpose the lattice properties on it by weighting each n-level transition by the known n-phonon density of states. Earlier, the simple Morse potential was used by Mills and Maradudin,[6] in a classical

calculation, to account for the frequency and temperature dependence of the absorption in the high-temperature limit. The model was extended to all temperatures by a quantum-mechanical calculation by Rosenstock[7] in which lattice dispersion was introduced via a Debye spectrum with no momentum-conservation rules. McGill *et al.*[3] have used the Morse potential to investigate the importance of the higher-order-moments mechanism.

The present treatment is brought appreciably closer to reality by the use of a realistic n-phonon (rather than 1-phonon) frequency distribution. The use of the Morse potential, which seems crude when interpreted as an approximation of a solid by a set of diatomic molecules, now appears only as a simple device for evaluating matrix elements in a model in which lattice properties are also properly treated. However, momentum conservation is still ignored.

The amount of anharmonicity in a Morse potential is mathematically related to the dissociation energy, and this we determine from the observed thermal expansion coefficient. As a result, the entire frequency and temperature dependence of the multiphonon spectrum can be calculated in a systematic way without adjustable parameters. We have applied this approach to nine alkali halides and three alkaline-earth fluorides. Best agreement with experiment is obtained for the heavier alkali halides. A number of predictions can be made about some of the details of the spectrum which have not yet been observed.

In Sec. II the calorimetric techniques of Harrington and Hass[11] for studying the temperature dependence of very low absorption coefficients are reviewed, along with new experimental results for the absorption of KCl at 10.6 μm. Arguments using temperature-dependence measurements for distinguishing between impurity and intrinsic absorption indicate that the absorption at 10.6 μm of a crystal grown at NRL is largely intrinsic. In Sec. III details of the theoretical model are discussed. In Sec. IV values for the parameters of the model are listed for the various materials studied, and related to the predictions of the Morse potential for thermal expansion and the temperature shift of spectral lines. In Sec. V these results are applied to calculate the frequency and temperature dependence of some cubic ionic crystals for which data are available and other substances for which no data are available, but interesting results are predicted. Some general aspects of these results are discussed in Sec. VI. A brief derivation of the absorption coefficient for a diatomic ionic gas is given in the Appendix.

II. EXPERIMENTAL TECHNIQUE

The absorption coefficients of KCl, NaCl, and NaF at a wavelength of 10.6 μm and in a temperature range from 300 to within 50 °K of the melting point have been studied. When the absorption coefficient is moderate (above 0.002 cm^{-1}), conventional double-beam spectrometers can be employed, and most of the previous experimental data referred to in Sec. V have been obtained in this manner. NaF was investigated by such a transmission arrangement. KCl and NaCl, on the other hand, were examined using a modification of the calorimetric method with a laser

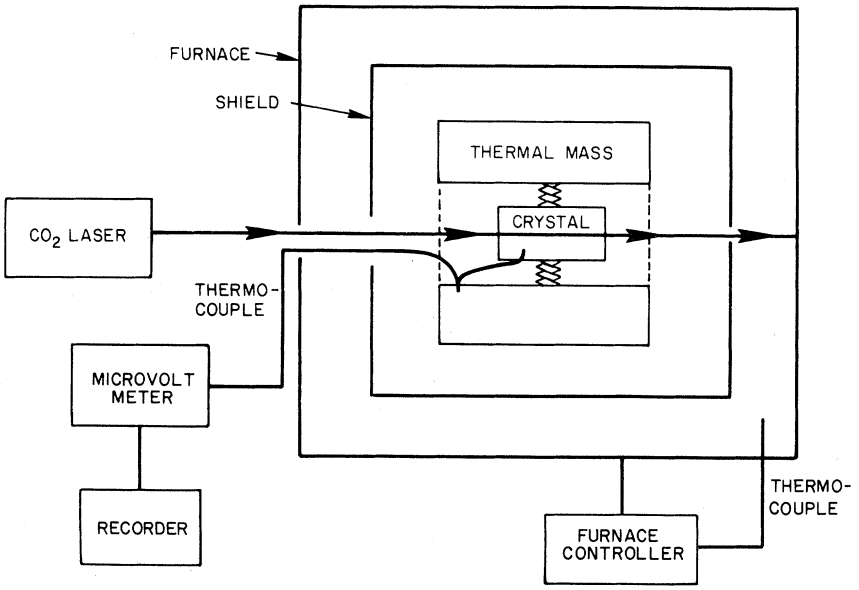

FIG. 1. Apparatus for laser calorimetric measurements above room temperature.

source. This involves the determination of small temperature rises (about 0.1 °K) in an oven operating up to 1000 °K, by an experimental technique that has not been discussed previously.

A schematic diagram of the apparatus is shown in Fig. 1. To ensure good thermal stability, the sample was mounted inside a thermal mass (5-cm-diam×10-cm-length stainless-steel cylinder) which was placed inside a stainless-steel box to minimize convection currents. This entire assembly was then loaded into a temperature-controlled furnace. Using this arrangement it was possible to achieve an ambient temperature stable to within 0.5 °K at 1000 °K. The temperature sensor to measure the thermal rise in the crystal on laser irradiation was a chromel-alumel thermocouple embedded in a small hole drilled in the crystal with sauerisen cement to ensure good thermal contact. The reference junction for this differential arrangement was the thermal mass.

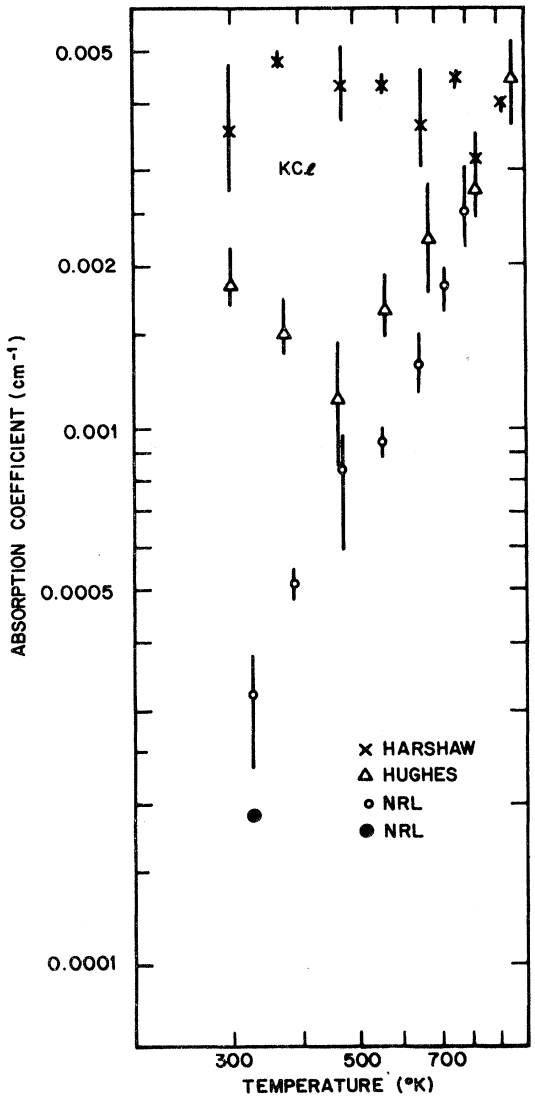

FIG. 2. Absorption coefficient of KCl at 10.6 μm for single crystals from various sources. Surface absorption has not been separated out.

Crystals from a number of different sources were employed for this investigation. The lowest absorption coefficients were obtained with crystals specially grown by P. H. Klein at this laboratory under conditions designed to minimize the introduction of oxygen-containing impurities which can give rise to absorption bands in the mid-infrared region. The results for KCl for crystals from various sources are illustrated in Fig. 2. The temperature dependence of the absorption at 10.6 μm is seen to be very sensitive to impurities. The lowest room-temperature absorption coefficient was obtained with a crystal grown in a CCl_4 reactive atmosphere.[12] The temperature dependence of the absorption for this crystal is monotonically increasing and this is anticipated for near-intrinsic absorption at room temperature. However, there is a surface absorption band at 9.5 μm, the wings of which can contribute to the total absorption at 10.6 μm. When this surface absorption is subtracted out, a bulk absorption coefficient of 0.000 08 cm^{-1} can be extracted, which is within experimental error of the value predicted by an extrapolation of data from higher frequencies based upon an exponential absorption law.[13,14] The surface absorption can be greatly reduced by chemical polishing.[15]

III. THEORY

We begin by collecting the needed formulas and shall discuss the physical model later in this section. The absorption coefficient of a gas of diatomic ionic molecules at temperature T (see Appendix) is

$$\beta(\nu, T) = \frac{4\pi^2\sigma e^2\Omega}{3\hbar c n_0 Z} \sum_m \sum_{n>0} |\langle m+n|r|m\rangle|^2 \times (e^{-E_m/kT} - e^{-E_{m+n}/kT})\delta(\Omega - E_{m+n}/\hbar - E_m/\hbar), \quad (1)$$

where $\nu = \Omega/2\pi$ is the frequency of the absorbed radiation, σ is the number of molecules per unit volume, e is the magnitude of the charge of the ions, $2\pi\hbar$ is Planck's constant, c/n_0 is the velocity of the light in the medium, k is Boltzmann's constant,

$$Z = \sum_m e^{-E_m/kT} \quad (2)$$

is the partition function, and E_m and $|m\rangle$ are the eigenvalues and eigenvectors of the Hamiltonian

for the vibrational motion of a single molecule. The Morse potential,[16]

$$V(r)=D(1-e^{-a(r-r_0)})^2\ , \tag{3}$$

will be used to determine $|m\rangle$ and E_m; it has energy levels

$$E_m=\hbar\omega(m+\tfrac{1}{2})[1-(1/j)(m+\tfrac{1}{2})],\quad m=0,1,2\ldots,m_{\max} \tag{4}$$

where $m_{\max}$ is the largest integer below $\frac{1}{2}(j-1)$, with

$$j=4D/\hbar\omega\ . \tag{5}$$

D is the dissociation energy, $\omega/2\pi$ is the classical frequency of small-amplitude oscillations of a particle of mass μ in the potential $V(r)$ and is related to the other parameters by

$$a=\omega(\mu/2D)^{1/2}\ . \tag{6}$$

Two parameters are required to define the Morse potential: D and a, related, respectively, to the depth and width of the potential well, or D and ω. Strictly speaking, r_0 is also an adjustable parameter, but the quantum mechanics of the Morse potential is independent of it.

The dipole-matrix elements $r_{mm'}=|\langle m|r|m'\rangle|$ in Eq. (1) are given by[17]

$$r^2_{m,m'}=\frac{(j-1-2m)(j-1-2m')}{[a(j-1-m-m')(m'-m)]^2}\,\frac{\binom{m'}{m}}{\binom{j-m-1}{m'-m}}\ , \tag{7}$$

where

$$\binom{m'}{m}$$

denotes the usual binomial coefficient and may be approximated as

$$r^2_{m+n,m}=\frac{(m+1)(m+2)\cdots(m+n)}{n!}\,\frac{\hbar}{2\mu\omega}\left(\frac{\hbar\omega}{4D}\right)^{n-1} \tag{8}$$

for low-lying levels (small m).

As $D\to\infty$, keeping ω fixed, $V(r)$ becomes a parabola, the second term in Eq. (4) goes to zero, and, from Eq. (8), only transitions to adjacent states are allowed (in agreement with the well-known[18] result for harmonic oscillators). Thus Eqs. (4) and (5) show that the parameter $\hbar\omega/4D$ is a measure of the amount of anharmonicity present. As usual, we shall refer to a transition involving states m and $m+n$ as an "nth-order" or "n-phonon" transition.

Many of the qualitative features of the frequency and temperature dependence of multiphonon absorption in solids can be interpreted using the above expressions for the Morse oscillator. For low temperatures ($T\ll\hbar\omega/k$) only transitions from the ground state, $m=0$, will contribute to β, which yields a sequence of δ-function lines, one line for each order n, with their intensities going as $(\hbar\omega/4D)^{n-1}$ [see Eq. (8)]. This dependence of β on the order of the transition reproduces the empirical law $\beta=Ae^{-\gamma(\Omega/\omega)}$, with $e^{-\gamma}=\hbar\omega/4D$. For higher temperatures the nth-order absorption will contain additional lines due to transitions from higher levels, $m\neq 0$ to $m+n$. These lines will be shifted to lower frequencies because, on account of the second term in Eq. (4), the spacing between higher levels is smaller. This provides a basis for the theoretical concept of thermal broadening. Experimental results so far indicate that the multiphonon spectrum is remarkably free of structure even at low temperatures.

The δ function in Eq. (1) implies an infinite lifetime of the excited states, as discussed in the Appendix. The customary Lorentzian line shape cannot be used in place of the δ function because it decays much to slowly. Including lifetime effects in a realistic way would be a difficult problem, which is avoided by using the δ-function description and *assuming* that the correct line shape decays faster than the matrix elements.

For high temperatures one obtains $\beta\propto T^{n-1}$ by summing over m in Eq. (1) with the assumption that the energy levels are given by their harmonic values. Including the level shifts causes a weaker temperature dependence because energy-conserving transitions in the upper levels are necessarily of higher order and therefore less probable.

The main virtue of the Morse potential is that it provides a convenient formalism for including the anharmonicity. Once the anharmonicity parameter is determined, the deviation of energy levels from their harmonic values is included implicitly through Eq. (4). By contrast, perturbation treatments insert this in an *ad hoc* way using the concept of a temperature-dependent density of states when actually, in a theory based on first principles, only population factors (not energy levels) depend on temperature.

The main problem with the Morse-potential treatment, or any independent-oscillator approach, for that matter, is adapting the formalism to quantitatively describe β for the solid in a way that is physically convincing. The harmonic frequency, ω in Eq. (4), can be interpreted on several levels of sophistication. The simplest is the single-oscillator picture (just discussed) in which ω is the reststrahl frequency. As we have seen, this

alone provides a qualitative explanation of the essential features of multiphonon absorption at high temperatures. An improvement is obtained by choosing a distribution of frequencies given by the one-phonon density of states of the solid, and integrating Eq. (1) over this distribution. This takes account of the fact that a solid, in contrast to a gas consisting of identical molecules, contains many, not just one, oscillator; but it does so in an *ex post facto* way. This approach has been employed by Rosenstock[7] using a Debye distribution.

A further improvement, both logically and quantitatively, is attained here by integrating first-order transitions over a one-phonon frequency distribution, second-order transitions over a two-phonon frequency distribution, etc. Explicitly, Eq. (1) becomes

$$\beta = \frac{4\pi^2\sigma e^2\Omega}{3\hbar c n_0} \sum_m \sum_{n>0} \int_0^\infty d\omega \, \frac{1}{Z(\omega)} r^2_{m+n,n}(\omega) \times (e^{-E_m(\omega)/kT} - e^{-E_{m+n}(\omega)/kT}) \rho_n(n\omega) \times \delta(\Omega - E_{m+n}(\omega)/\hbar + E_m(\omega)/\hbar) , \quad (9)$$

where σ is now the oscillator density of the solid and ρ_1 is normalized to unity,

$$\int_0^\infty \rho_1(\omega)\, d\omega = 1 . \quad (10)$$

Given ρ_1, we approximate the higher-order distributions by

$$\rho_n(\omega'') = \int_0^\infty d\omega \int_0^\infty d\omega' \, \rho_{n-1}(\omega')\rho_1(\omega)\delta(\omega'' - \omega' - \omega) \quad (11)$$

using an iteration procedure beginning with $n=2$. We recognize ρ_n in Eq. (11) as the probability of finding n phonons in the lattice whose energies add up to ω''. Thus, in the present approach, the fact that transitions from levels m to $m+n$ involve physically the creation of n lattice phonons is properly weighted. The Morse-potential model now serves the sole purpose of providing a convenient tool for computing the strength of the anharmonic interaction in a physically reasonable way. To be sure, this still neglects wave-vector conservation and "difference processes" in which some phonons are destroyed as well as created. Proper account of the former would replace Eq. (11) by complicated multiple integrals over wave-vector space; we can argue that detailed effects would probably average out for higher-order transitions. Difference processes must, on the average, be of higher order than the "summation processes" we consider, and will therefore make a relatively small contribution to β.

The quantity $\rho_1(\omega)$ is the "measured" one-phonon density of states of the solid at $T=0$ corrected to eliminate anharmonic effects which measurements necessarily contain. This is not usually available and so the density of states is obtained from lattice-dynamical calculations in the harmonic approximation in which the parameters are chosen to give a good fit to neutron-scattering measurements taken at some temperature $T>0$. ρ_1 must then be adjusted to its $T=0$ value (thermal correction) and further modified to account for the fact that, according to Eq. (4), even at $T=0$ the measured frequencies correspond to $(E_1 - E_0)/h$ rather than the harmonic frequency $\omega/2\pi$ (anharmonic correction). These corrections produce mainly a change in scale of ρ_1 and are included because the multiphonon absorption is sensitive to this.

Recall that two parameters, the harmonic frequency and the dissociation energy, are required to define the Morse potential. Integrating over the appropriate frequency distribution accounts for the parameter ω. We take the dissociation energy to be independent of ω and determine it by fitting to expansion-coefficient data as discussed below.

IV. INPUT

Values for the oscillator density σ, index of refraction n_0, and the reduced mass μ of the materials considered are listed in Table I. The oscillator density for the alkali halides is $24/a_0^3$, and for the fluorite-structured materials $36/a_0^3$, where a_0 is the size of the cubic unit cell. The factors 24 and 36 result from the fact that 8 and 12 ions are contained in the cubic unit cell and the corresponding numbers of modes are three times these numbers. The frequency dependence of n_0 is negligible, as is the temperature dependence of σ and n_0. The full ionic charge of one electron is taken for all alkali halides and two electrons for the fluorite-structured materials. For the alkali halides the reduced mass is the usual $\mu = m_+ m_-/(m_+ + m_-)$, while for the fluorites we choose $\mu = 2 m_+ m_-/(m_+ + 2 m_-)$.

The harmonic-frequency distribution $\rho_1(\omega)$ is obtained from published density-of-states calculations (Refs. 19–26) as follows:

$$\rho_1(\omega) = \rho(\omega'), \quad (12)$$

where

$$\omega = (1 + \Delta)\omega' \quad (13)$$

and $\Delta = \Delta_T + \Delta_A$ is the sum of the temperature and anharmonic corrections discussed above. A histogram form containing ~20 increments was used for $\rho(\omega)$ with the values taken from the above references. Results for KF and KI (Figs. 3 and 4) illustrate the dependence of $\rho_n(\omega)$ and n. We see that detailed structure tends to disappear as n

TABLE I. Lattice constants, oscillator densities, indices of refraction, and reduced masses of the compounds treated.

	LiF	NaF	KF	NaCl	KCl	RbCl	NaBr	KBr	KI	CaF_2	SrF_2	BaF_2
a_0 (Å)	4.02	4.62	5.34	5.62	6.28	6.58	5.96	6.58	7.06	5.46	5.80	6.20
σ (Å^{-3})	0.369	0.243	0.158	0.135	0.097	0.084	0.113	0.084	0.068	0.221	0.185	0.151
n_0	1.30	1.25	1.36	1.45	1.45	1.49	1.64	1.50	1.60	1.37	1.44	1.40
μ (amu)	5.12	10.4	12.8	13.9	18.4	24.8	17.9	26.2	29.8	19.5	26.5	29.7

increases, with ρ_n becoming more and more Gaussian in shape. Apparently the gap in the density of states for KI causes this to happen much more slowly than for materials such as KF, which have no gap. This shows that the central limit theorem is not appropriate for all materials, especially those which have a gap in their density of states, as noted by Sparks.[2b] References for the density-of-states functions used in these calculations are given in Table II along with the thermal and anharmonic correction factors. The thermal corrections were made assuming a linear temperature dependence of the peak of the reststrahl line using the data of Lowndes and Martin[27] and Denham *et al.*[28] The anharmonic correction depends on the value of $\hbar\omega/4D$ [see Eq. (4)]. The values of Δ_A listed in Table II are those appropriate to the frequencies of $T=0$ reststrahl lines and the dissociation energies obtained from expansion-coefficient data.

To fix the dissociation energy we use the measured temperature dependence of the expansion coefficient of the solid. The coefficient of linear thermal expansion of a diatomic molecule is given by

$$\alpha = \frac{1}{r_0}\frac{d\langle r\rangle}{dT} \quad , \tag{14}$$

where r_0 is the equilibrium separation and

$$\langle r\rangle = \sum_m \langle m|\, r\,|m\rangle \frac{e^{-E_m/kT}}{Z} \tag{15}$$

is the thermal average of r. For the Morse potential E_m is given by Eq. (4) and the matrix elements by[17]

$$\langle m|\, r\,|m\rangle = (1/a)[ar_0 + 2\ln(2D/\hbar\omega) - \Psi(t+1)], \tag{16}$$

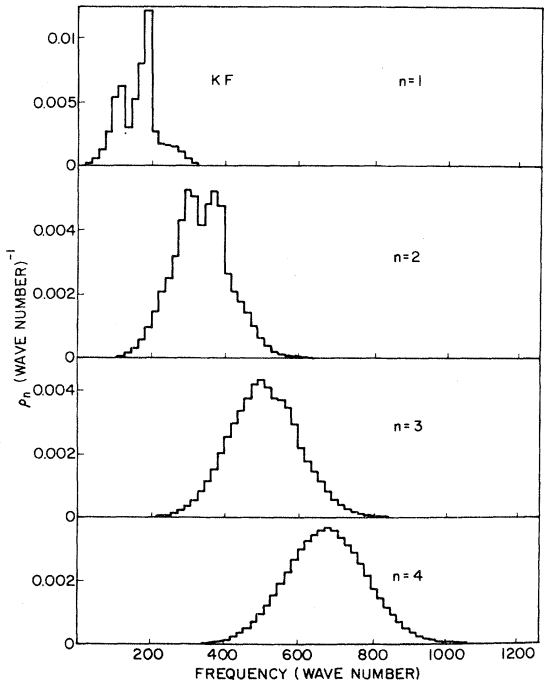

FIG. 3. Normalized n-phonon frequency distribution $\rho_n(\nu)$ for KF, with no anharmonic or thermal corrections included ($\Delta=0$).

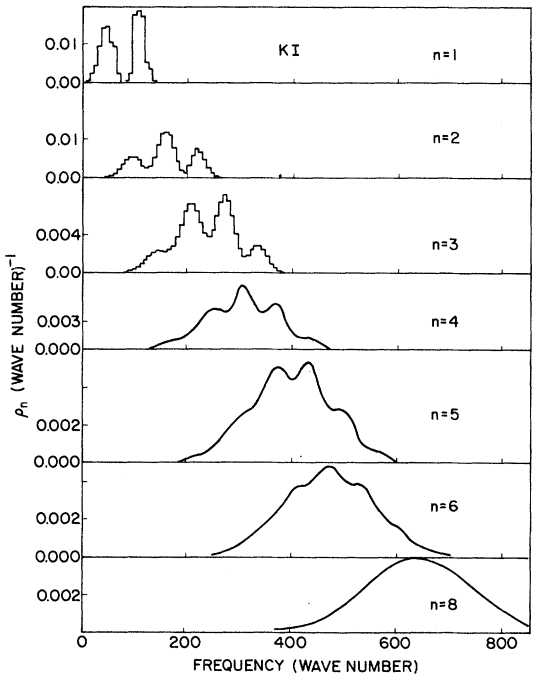

FIG. 4. Normalized n-phonon frequency distribution $\rho_n(\nu)$ for KI, with no anharmonic or thermal corrections included ($\Delta=0$).

TABLE II. References for the density of states $\rho(\omega)$ at temperature T and the thermal and anharmonic corrections for the compounds treated.

	LiF	NaF	KF	NaCl	KCl	RbCl	NaBr	KBr	KI	CaF_2	SrF_2	BaF_2
Reference for $\rho(\omega)$	22	23	19	21	21	20	21	21	21	26	25	24
T (°K)	300	300	300	80	80	80	80	80	80	300	300	300
Δ_T	0.043	0.063	0.039	0.022	0.017	0.020	0.022	0.020	0.019	0.034	0.034	0.032
Δ_A	0.034	0.032	0.023	0.023	0.020	0.012	0.018	0.015	0.014	0.050	0.031	0.029

where

$$t = j - 2m - 2 \tag{17}$$

and Ψ is the logarithmic derivative of the Γ function:

$$\Psi(u) = -C + 1 + \tfrac{1}{2} + \tfrac{1}{3} + \cdots + 1/u\ , \tag{18}$$

$C = 0.577215$ (Euler's constant).

Using the above expressions, values for ω and D have been determined for a number of alkali halides and alkaline-earth fluorides by choosing r_0 to be the nearest-neighbor separation and fitting α and $d\alpha/dT$ to measured values[29-31] at room temperature. These results are listed in Table III. Using these values for ω and D the temperature dependence of the expansion coefficients of these materials has been compared with experiment. The agreement is very good for a wide variety of compounds, and a typical result is shown in Fig. 5. The uncertainties in ω and D obtained in this manner appear to be ~10 and 25%, respectively; e.g., fitting to the measurements of Ref. 30 for NaCl yields $\omega/2\pi = 148$ and $D/h = 3300$ wave numbers at $T = 300$ °K and $\omega/2\pi = 140$ and $D/h = 3560$ at $T = 350$°K, while fitting to the corresponding values in Ref. 29 yields $\omega/2\pi = 126$ and $D/h = 4190$ and $\omega/2\pi = 117$ and $D/h = 4620$, respectively.

Another quantity from which D might have been determined is the temperature dependence of the peak of the reststrahl line. The minimum in the transmission spectrum occurs at the frequency where the absorption coefficient is maximum. For $T = 0$ this is clearly at $\Omega = (E_1 - E_0)/\hbar$. At nonzero temperatures transitions between higher levels contribute to the absorption coefficient and, because of Eq. (4), cause the peak to shift to lower frequencies. From Eqs. (1) and (8) we see that near the fundamental absorption band

$$\beta \propto \sum_m m(e^{-E_m/kT} - e^{-E_{m+1}/kT}) f_m(\Omega)\ , \tag{19}$$

where $f_m(\Omega)$ is the line shape for transitions between the mth and $m+1$ levels. The precise amount of the shift depends upon the choice for f_m as well as the temperature and amount of anharmonicity. Assuming f_m is Gaussian with a 10% half-width and taking $\omega/2\pi$ and D to be 160 and 4000 wave numbers yields a shift of 2.8% upon going from $T = 0$ to room temperature. Typical measured shifts in the reststrahl line for alkali halides are 4–8%.[27] Thus using dissociation energies determined from the expansion coefficient yields temperature-dependent shifts in the reststrahl line that are too low by about a factor of 2. Dissociation energies obtained from expansion-coefficient data were therefore used in our calculation of multiphonon absorption, as they yield significantly better results.

V. RESULTS

The temperature and frequency dependence of the multiphonon absorption in a number of alkali halides and alkaline-earth fluorides has been calculated according to the procedures given in Secs. III and IV. For convenience in discussion, the calculations for the frequency dependence of

TABLE III. Values for the frequency and dissociation energy of a Morse oscillator obtained by fitting to expansion-coefficient measurements (α and $d\alpha/dT$ at room temperature) obtained from the indicated references.

	LiF	NaF	KF	NaCl	KCl	RbCl	NaBr	KBr	KI	CaF_2	SrF_2	BaF_2
$10^5\alpha$ (°K)$^{-1}$	3.29	3.29	3.17	3.88	3.68	4.02	4.19	3.76	4.00	1.94	1.82	1.88
$10^8 d\alpha/dT$ (°K)$^{-2}$	4.76	3.42	2.83	3.50	3.41	2.09	3.24	2.82	3.42	4.13	2.33	2.60
$D/\hbar$ (wave number)	4950	4610	4660	4190	3950	5650	4380	4350	3930	3130	4030	3600
ν (wave number)	277	189	154	126	109	65	94	80	71	285	212	199
Reference	30	29	29	29	29	30	29	29	29	31	31	31

the absorption at three temperatures 50, 300, and 600 °K have been carried out and are shown in Fig. 6 for the potassium halides, Fig. 7 for LiF, NaF, and NaCl, and Fig. 8 for the alkaline-earth fluorides CaF_2, SrF_2, and BaF_2. Experimental data where available have been included. The temperature dependence of the absorption at certain selected frequencies has been calculated for the alkali halides LiF, NaF, NaCl, KCl, and KBr and compared with available experimental data in Fig. 9.

Before considering these results in detail, a few general comments are in order. On the whole, the calculations yield a nearly uniform exponential dependence of the absorption coefficient as a function of frequency. There is some small multiphonon structure which increases for the heavier compounds, as seen in Fig. 6 for the potassium halides, and the underlying reason for this will be discussed later. No evidence for structure can be found in the experimental data. Both the frequency- and temperature-dependence data are consistent with the calculations, although the agreement in the temperature dependence is better for the heavier compounds than for the lighter ones.

A. Potassium halides

The calculated and observed frequency dependence of the absorption coefficient is shown in Fig. 6. As is evident from the calculations, and as will be discussed later, there is essentially no multiphonon structure for KF and considerable multiphonon structure for KI. Unfortunately, no experimental data could be found for comparison.

KCl. The room-temperature absorption data in the multiphonon region for a number of samples of KCl have been obtained by Deutsch[13] and are shown in Fig. 6(b). Included also is that value at 10.6 μm obtained in a laser calorimeter by Hass *et al.*[12] with a chemically polished[15] crystal grown in a CCl_4 reactive atmosphere. The bulk absorption coefficient at this wavelength is about 0.000 08 cm^{-1}, which is consistent with that obtained by an extrapolation of the intrinsic absorption from lower frequencies. Similar results have been reported by Deutsch.[14] The temperature dependence of the absorption at 10.6 μm has been studied by Harrington and Hass[11] on crystals in which the room-temperature absorption was dominated by impurities. The temperature dependence of a pure crystal of KCl in which the room-temperature absorption is believed to be intrinsic is shown in Figs. 2 and 9(d). The latter shows fairly good agreement between experiment and theory. A problem in KCl is that there can be both surface and bulk absorption near 10.6 μm. By use of pure crystals, chemical polishing, and heating in vacuum followed by *in situ* emittance measurement, Stierwalt and Hass[32] have found that the surface absorption can be largely eliminated.

KBr. The absorption coefficient of KBr in the multiphonon region has been collected by Deutsch[13] and is slightly lower than measurements of those of Califano and Czerny.[33] Deutsch's frequency data fit the calculations very closely [Fig. 6(c)].

The temperature-dependence data of Barker[34] at two frequencies have been compared with the calculations in Fig. 9(e). On the whole the agreement is satisfactory.

B. Alkali halides: LiF, NaF, and NaCl

LiF. Some data exist for both the frequency and temperature dependence of absorption of LiF. The room-temperature data have been collated by Deutsch[13] and are shown in Fig. 7(a). Some small multiphonon structure is predicted, but is not evident in the data. The structure in the high-temperature calculations is due to limitations of the Morse potential resulting from a finite number of levels, as discussed in Sec. VI. Temperature-dependence measurements have been given by Barker[34] and Klier[35] with those of Klier markedly lower in magnitude, as seen in Fig. 9(a). In both cases the observed variation is greater than that predicted by the model.

NaF. The widest range of data for the frequency and temperature dependence of absorption exists for NaF. The room-temperature absorption has been reported in the multiphonon region by Klier[35] and McNelly and Pohl[36] for crystals grown in an

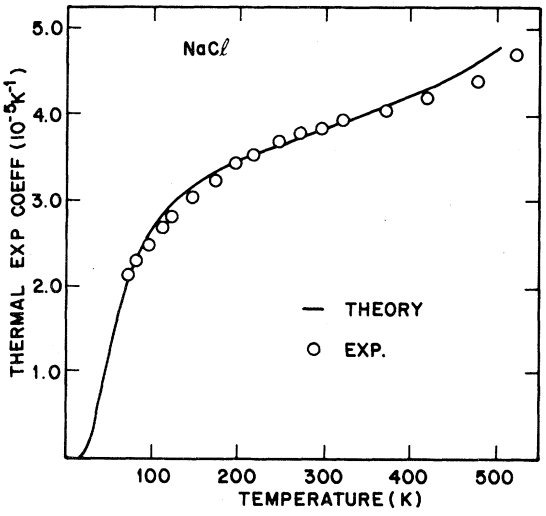

FIG. 5. Comparison of the experimental and theoretical temperature dependence of the linear thermal expansion coefficient of NaCl.

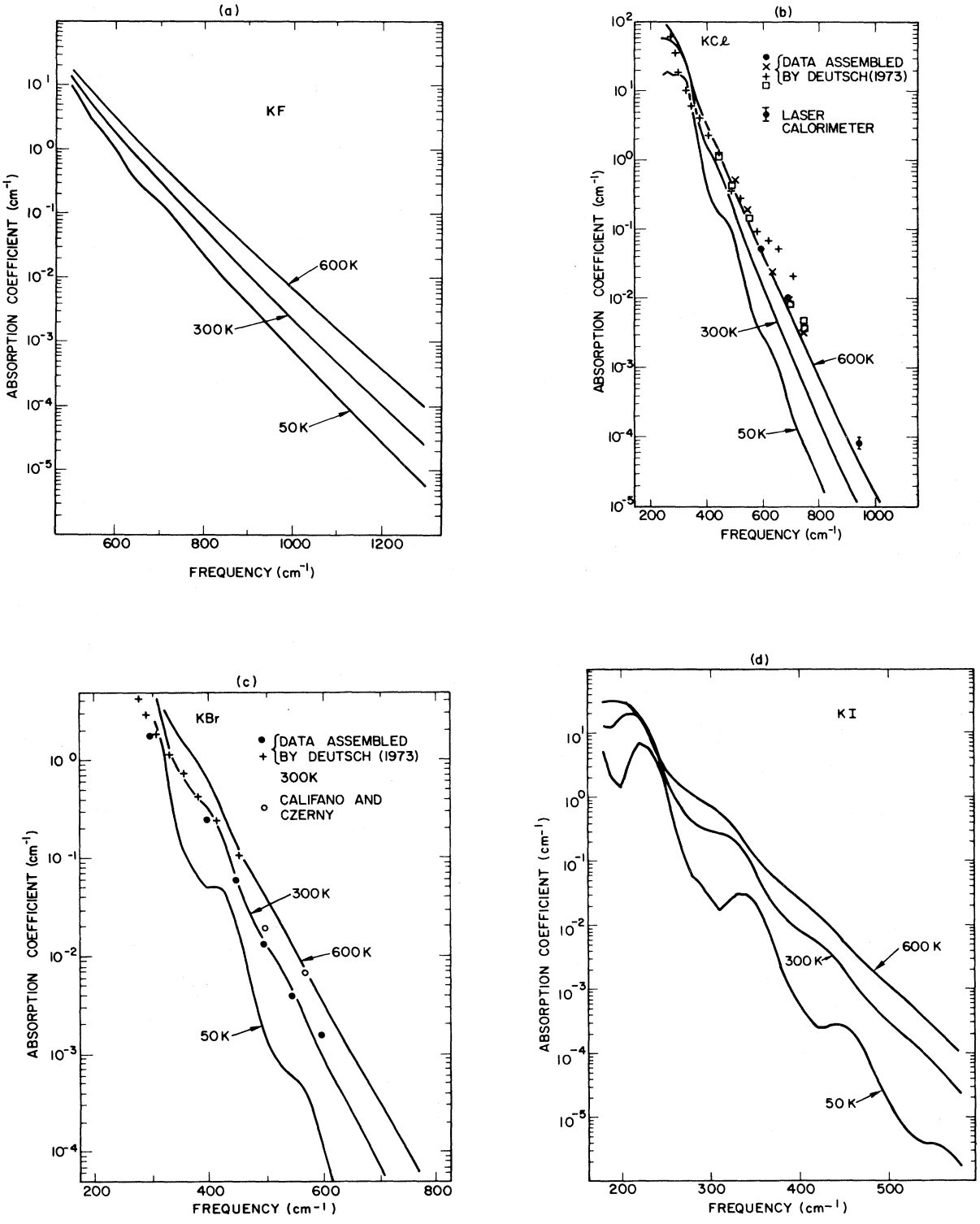

FIG. 6. Theoretical and experimental results for the frequency dependence in the multiphonon region of the absorption coefficients of the potassium halides at $T = 50$, 300, and 600 °K. (a) KF; (b) KCl; (c) KBr; (d) KI.

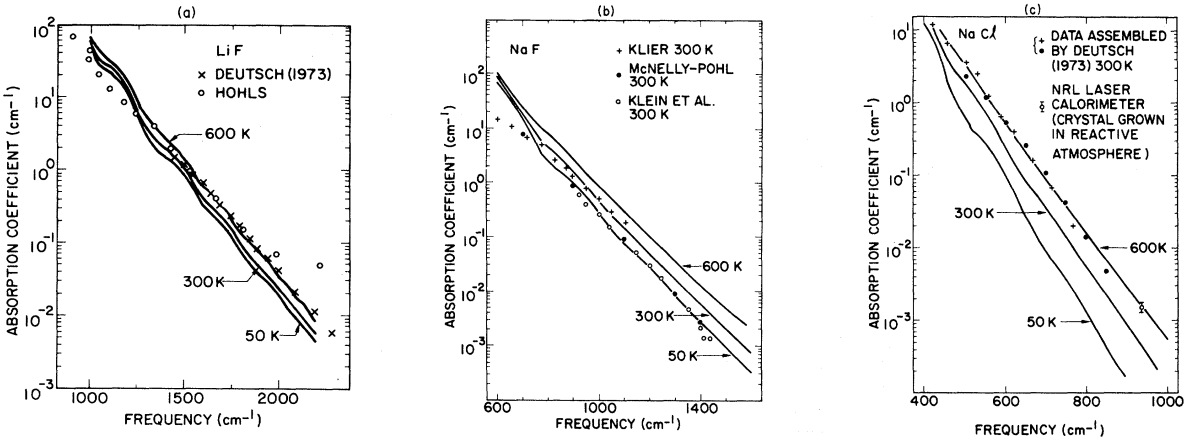

FIG. 7. Theoretical and experimental results for the frequency dependence in the multiphonon region of the absorption coefficients of the alkali halides LiF, NaF, and NaCl at $T = 50$, 300, and 600 °K. (a) LiF; (b) NaF; (c) NaCl.

argon atmosphere, and by Klein *et al.*[37] for a crystal grown in an argon atmosphere from specially purified starting material. The data are shown in Fig. 7(b) with Klier's results somewhat higher than the others. Some evidence for impurity absorption in oxygen-grown crystals reported by Pohl and Meier[38] and an absorption band near 1600 cm^{-1} can be observed in the emittance spectrum of one crystal and is absent in another. The calculated results are somewhat higher than the observed results. Some multiphonon structure is predicted at low temperatures, but this is not very pronounced.

The temperature dependence at 10.6 μm (943 cm^{-1}) has been reported by Harrington and Hass[11] and Pohl and Meier.[38] Results from 700 to 1400 cm^{-1} have been reported by McNelly and Pohl.[36] Figure 9(b) shows that these experimental values increase somewhat more rapidly than the calculations.

NaCl. The dependence of the room-temperature data on the absorption coefficient for NaCl as a function of frequency has been obtained by Deutsch[13] and his data fit on the same exponential curve as earlier data of Mentzel[39] and subsequent data of Califano and Czerny.[33] A measurement at 10.6 μm on an NaCl crystal grown in a reactive atmosphere and chemically polished gave an absorption coefficient of 0.0013 cm^{-1} which lies on the curve. The surface absorption was negligible. The temperature dependence at 10.6 μm was determined by Harrington and Hass[11] and at lower frequencies by Barker.[34] Some of these data are compared with the calculations in Fig. 9(c). On the whole, the

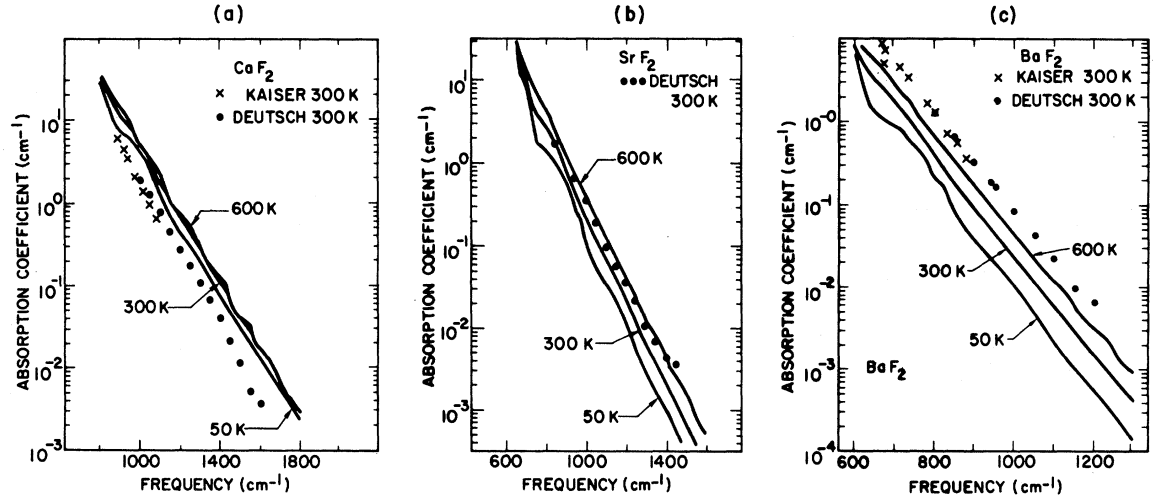

FIG. 8. Theoretical and experimental results for the frequency dependence in the multiphonon region of the absorption coefficients of the alkaline-earth fluorides at $T = 50$, 300, and 600 °K. (a) CaF_2; (b) SrF_2; (c) BaF_2.

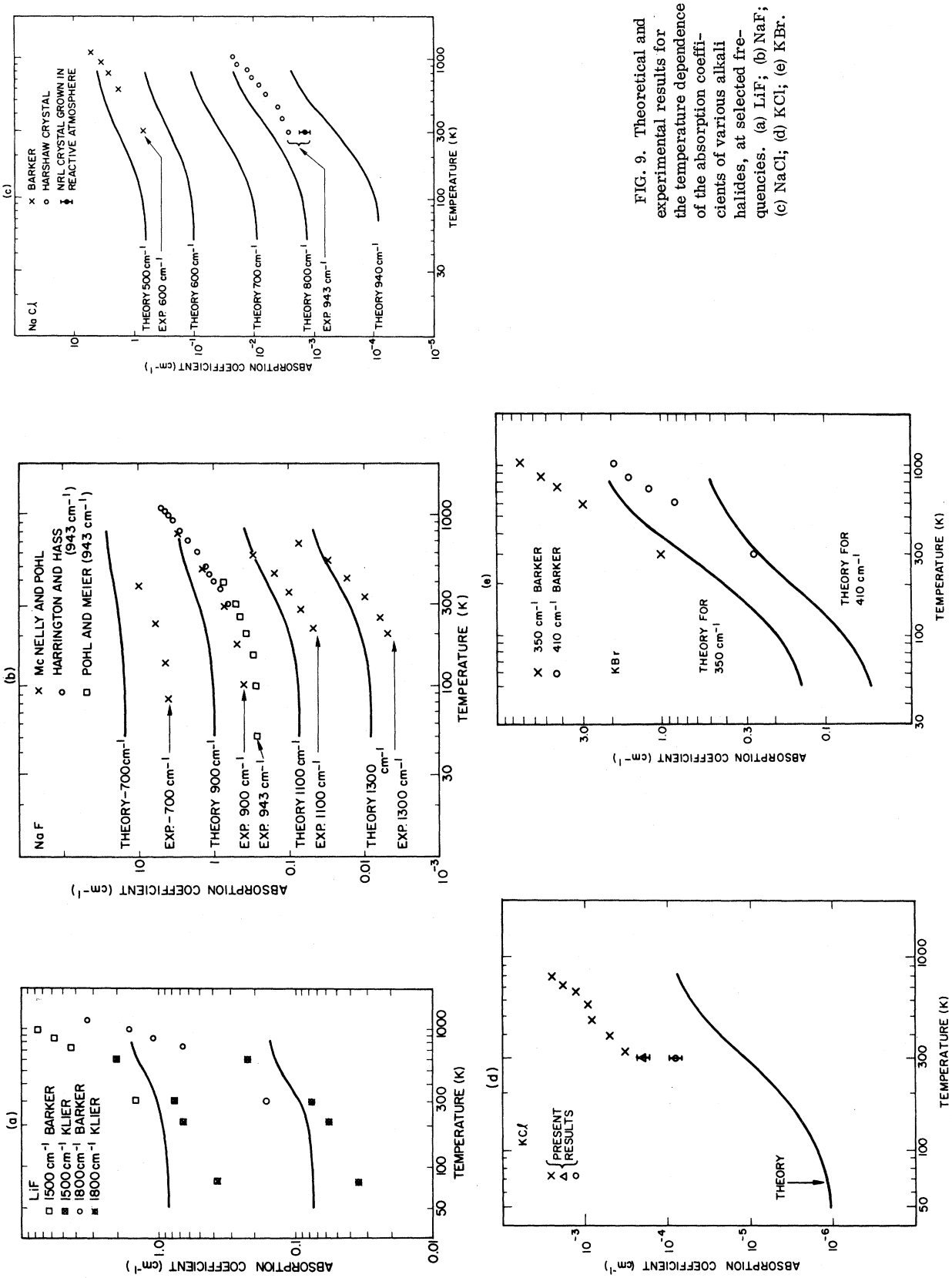

FIG. 9. Theoretical and experimental results for the temperature dependence of the absorption coefficients of various alkali halides, at selected frequencies. (a) LiF; (b) NaF; (c) NaCl; (d) KCl; (e) KBr.

agreement between the calculated and experimental values is fairly good.

C. Alkaline-earth fluorides: CaF_2, SrF_2, and BaF_2

The absorption coefficient in the multiphonon region for the alkaline-earth fluorides has been given by Kaiser *et al.*[40] and Deutsch.[13] The data are collected in Fig. 8. The agreement between calculation and experiment is good for SrF_2 and not as good for CaF_2 and BaF_2. Since experiment is lower than calculation for CaF_2, about the same for SrF_2, and higher for BaF_2, this suggests that the agreement for SrF_2 may be somewhat fortuitous. Since the optical frequencies compared to the well depth are higher for these materials (and also for LiF and NaF), some wiggles that are an anomaly of the calculation appear at high temperatures, as explained in Sec. VI. Temperature-dependence data in the literature[41] were not sufficiently extensive for comparison with experiment.

VI. DISCUSSION

The theoretical results for low temperatures reveal structure in the frequency dependence which is associated with the order of the dominant transitions. The most structure tends to occur for the heavier compounds; e.g., compare the spectra for the potassium halides. Calculations for NaBr and RbCl (not shown) are similar to those for KCl and KBr, respectively, and further support the trend of more structure for heavier compounds. Two factors must be considered in explaining these results. First of all, the dissociation energies we obtain from expansion-coefficient data are roughly the same for all these materials, but $\omega \sim \mu^{1/2}$. The anharmonicity goes as $\hbar\omega/4D$, and the heavier compounds are therefore less anharmonic. From Eq. (8) this results in a more abrupt change in the absorption in heavier compounds upon going from an n- to an $n+1$-dominated region. Second, we must consider the effect of structure in the frequency distributions ρ_n on the absorption spectrum. We illustrate this by comparing the results for KF and KI. For KF (Fig. 3) we see that at the frequency beyond which ρ_n becomes small (in the high-frequency wing), ρ_{n+1} is a relatively smoothly decaying function for $n>2$, and this in turn yields a structure-free multiphonon spectrum at low temperatures. On the other hand, for KI (Fig. 4), a significant amount of structure remains in ρ_{n+1} after $\rho_n \to 0$ for n out to about 5 or 6. The effect of this is clearly evident in the absorption spectrum [see Fig. 6(d)]. For example, the slight shoulder ~ 280 cm^{-1} is due to the third peak in ρ_3, while the large band at ~ 340 cm^{-1} is due to the adjacent highest frequency peak in ρ_3. For lower frequencies second-order processes dominate and therefore the effect of structure in the low-frequency end of ρ_3 is not visible. The higher-order bands are each due to the outermost peak in ρ_n.

As the temperature is raised, contributions from $m>0$ [see Eq. (9)] tend to remove whatever structure exists at low temperatures. If the temperature is too high, artificial structure can arise due to a limitation of the model imposed by the finite dissociation energy. We have ignored transitions to the continuum of states of a Morse oscillator that lie above the dissociation energy. At high enough temperatures transitions to these states are no longer improbable and the calculations are not reliable.

Experimental results so far show little evidence of structure due to multiphonon ($n>3$) effects. However, these measurements have for the most part been done at room temperature and for materials which theoretically show little structure.

Except for the structure at low temperatures the spectrum in nearly exponential and may be approximated by

$$\beta = A e^{-\gamma(\nu/\nu_0)} , \tag{20}$$

where A and γ are constants of the material which depend on temperature. ν_0 is some characteristic frequency of the solid which we choose, following Deutsch,[13] to be the longitudinal optic frequency. Values for A and γ have been determined by least-squares fitting the calculated spectrum in the three- and higher-phonon region to that of Eq. (20). These results are listed in Table IV along with values obtained from room-temperature experimental results. We see that calculated values agree to within $\sim 50\%$ for A and $\sim 10\%$ for γ of the corresponding experimentally determined values. The better agreement for γ is somewhat superficial since γ occurs in the exponential of Eq. (20). If we write $\beta = A(B)^{\nu/\nu_0}$ [which is more realistic in view of Eq. (8)] then the agreement in B is only about 50%.

From experimental results thus far available the following qualitative picture of the temperature dependence of multiphonon absorption emerges (see Fig. 9). At low temperatures ($T \lesssim 100$ °K) the absorption is nearly constant, while at high temperatures ($T \gtrsim 400$ °K) the absorption goes as T^x, where x increases with increasing frequency. Interestingly enough, this high-temperature description seems to hold even through melting.

The present theory agrees well with this description in the low- and intermediate-temperature ranges, but for high temperatures the theory

TABLE IV. Experimental and theoretical values for A and γ in the approximate expression, $Ae^{-\gamma\nu/\nu_0}$, for the absorption coefficient.

		Expt. ($T=300$ °K)		Theory					
				A (cm^{-1})			γ		
	ν_0 (cm^{-1})	A (cm^{-1})	γ	$T=50$ °K	$T=300$ °K	$T=600$ °K	$T=50$ °K	$T=300$ °K	$T=600$ °K
LiF	673	21 300	4.4	47 300	51 500	68 400	4.97	4.92	4.88
NaF	425	41 000	5.0	27 300	27 900	28 600	4.89	4.68	4.42
NaCl	268	24 300	4.8	16 600	15 800	14 400	5.45	4.96	4.58
NaBr	206			8840	10 000	11 100	5.55	4.99	4.54
KF	318			17 400	18 100	16 900	5.39	5.04	4.68
KCl	213	8700	4.2	8200	8690	8150	5.19	4.65	4.29
KBr	166	6080	4.2	7710	9590	7860	4.97	4.43	4.04
KI	138			3940	8510	7840	5.22	4.70	4.34
RbCl	172			8960	11 300	8680	5.71	5.06	4.56
CaF_2	475	105 700	5.1	30 800	46 100	68 900	4.36	4.39	4.51
SrF_2	384	22 500	4.4	23 700	29 600	35 900	4.67	4.52	4.37
BaF_2	330	49 600	4.8	23 200	30 100	33 600	4.83	4.63	4.45

breaks down again, because of the finite dissociation energy. For the ultimate extreme, $T\to\infty$, all levels of the well are equally populated and there is no absorption. This causes the artificial "leveling off" of the temperature dependence at high temperatures, seen in Figs. 9(a)–9(e). For this reason it is difficult to obtain values of x for comparison with experimental results. Nevertheless, such a comparison is made in Table V by taking the theoretical values from the regions of maximum slope in $\log\beta$ versus $\log T$. Uncertainties in the experimental values were obtained by visually inspecting the data listed in Figs. 9(a)–9(e) to determine extremum values.

The theory tends to underestimate the value of x with the poorest agreement for the lighter compounds. The reason for this is at least partly due to the artificial depression of the temperature dependence at high temperatures discussed above. The knee in the curves between the constant low-temperature and T^x high-temperature dependences occurs at higher temperatures for the lighter compounds and therefore the artificial depression sets in relatively sooner, causing a greater reduction in the value of x.

It is interesting to analyze the absorption at a given frequency in terms of the order of the dominant processes. At low temperatures the absorption tends to be dominated by a single order. As the frequency is increased the dominant contribution is taken over continuously, but in some cases rather abruptly, by the next higher order. As explained above, the abruptness of this change depends on the amount of anharmonicity as well as structural details in $\rho_n(\Omega)$, and accounts for the varied amount of structure in the multiphonon absorption spectra of the potassium halides at low temperatures. As the temperature is raised contributions from higher orders becomes increasingly important, resulting in thermal broadening. This is illustrated in Fig. 10, where we have plotted the percentage of the total absorption in KCl at 10.6 μm due to the various orders as a function of temperature. At $T=0$, ~80% of the total absorption is due to fifth-order transitions, while at $T=600$ °K each contribution is less than 30% and the contribution from the fifth order is only 4%.

In summary, the frequency and temperature dependence of the multiphonon absorption has been calculated via the independent-oscillator model with an exactly solvable anharmonic potential (Morse). The depth of the well was evaluated by fitting to the observed thermal expansion coefficient and lattice dispersion was introduced via a multiphonon density of states. This approach allows the calculation to be carried out in a systematic way for many crystals with no adjustable parameters. These calculations were compared with existing data and some new data for the alkali halides and alkaline-earth fluorides. Good agreement was obtained, especially for the heavier alkali

TABLE V. Comparison of experimental and theoretical values of x in the high-temperature expression $\beta\propto T^x$ for the absorption coefficient.

Material	ν (cm^{-1})	x Expt	x Theory
LiF	1500	1.5± 0.2	0.58
	1800	2.8± 1.2	0.63
NaF	943	1.6± 0.3	0.96
	1100	2.2± 0.4	1.17
	1300	2.9± 0.8	1.29
NaCl	600	1.7± 0.3	1.17
	943	2.0± 0.4	2.00
KCl	943	3.0± 0.8	2.44
KBr	350	1.6± 0.2	1.38
	410	1.6± 0.2	1.18

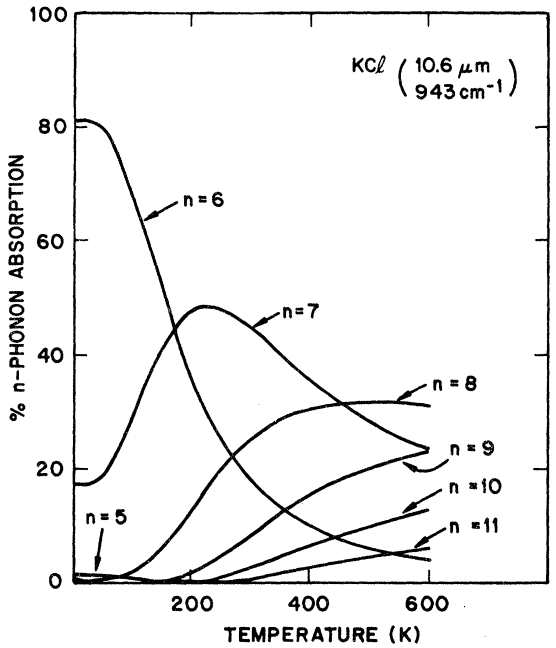

FIG. 10. Theoretical results for the percentage of the total absorption in KCl at 10.6 μm due to processes of order $n=5-11$ as a function of temperature.

halides. In addition, low-temperature structure in the multiphonon absorption, which has not yet been observed, was predicted for a number of compounds.

ACKNOWLEDGMENTS

The authors would like to thank D. L. Mills for a number of fruitful discussions, P. H. Klein for a number of pure crystals, and J. W. Davisson for discussion of chemical polishing and a number of measurements.

APPENDIX: ABSORPTION COEFFICIENT FOR A DIATOMIC IONIC GAS

The procedure for deriving the absorption coefficient of a material according to standard quantum mechanics is not new. However, a somewhat detailed derivation is needed here to clarify problems arising in our particular model.

The Hamiltonian for a point particle with mass m, charge e, and zero spin in an electromagnetic field is[42]

$$H=\frac{1}{2m}\left(\vec{p}-\frac{e}{c}\vec{A}\right)^2+e\varphi, \tag{A1}$$

where φ and $\vec{A}$ are the scalar and vector potentials describing the electromagnetic field and $\vec{p}$ is the conjugate momentum which may be considered as the sum of the radiation and mechanical momentum of the particle. The units in Eq. (A1) are Gaussian; when m is in g, e in statC, $\vec{p}$ in g cm/sec, and φ and $\vec{A}$ in statC/cm, then H is in erg. From Eq. (A1) the vibrational part of the Hamiltonian for a diatomic ionic molecule in an external field, $\vec{A}=\vec{A}_0\cos(\Omega t)$, simplifies to

$$H=H_0+H'(t), \tag{A2}$$

where

$$H_0=(p^2/2\mu)+V(r) \tag{A3}$$

and

$$H'(t)=(e/\mu c)pA_0\cos\theta\cos(\Omega t), \tag{A4}$$

where θ is the angle between p and A_0 and μ is the reduced mass. The field $A_0\cos(\Omega t)$ describes electromagnetic radiation in the dipole approximation (infinite wavelength compared to the size of the molecule). The scalar potential becomes simply the Coulomb interaction (radiation gauge) and is contained in $V(r)$ along with a short-range repulsive interaction. Contributions to A due to motion of the ions have been neglected, as they are small compared to any reasonable light intensity. Also, the A^2 term is neglected, as it is small except for very intense light ($\sim 10^{12}$ W/cm^2).

We let $|n\rangle$ and $E_n=\hbar\omega_n$, $n=0,1,2,\ldots$, denote the eigenvectors and eigenvalues of H_0. Given that at time $t=0$ the molecule is in state m, the probability that a measurement at a later time t will show it to be in state n, is, to first order in H', given by[43]

$$W_{m\to n}(t)=\left|\frac{i}{\hbar}\int_0^t e^{-i\omega_n(t-t')}\langle n|H'(t')|m\rangle \times e^{-i\omega_m t'}\,dt'\right|^2. \tag{A5}$$

This is a very good approximation because H'/H_0 is very small ($H'\sim H_0$ requires light intensities on the order of 10^{15} W/cm^2). Substituting Eq. (A4) with $p=(\mu/i\hbar)[r,H_0]$ and taking the limit as $t\to\infty$ yields

$$W_{m\to n}(t)=\frac{e^2A_0^2\cos^2\theta}{4c^2\hbar^4}(E_n-E_m)^2|\langle n|r|m\rangle|^2 \times 2\pi t\,\delta(\omega_n-\omega_m-\Omega) \tag{A6}$$

for $E_n>E_m$, together with $W_{n\to m}=W_{m\to n}$. A difficulty arises in taking the limit $t\to\infty$ because W is a probability and cannot be greater than 1. This may be "corrected" by assuming that the system will decay naturally from n to m according to $e^{-t/\tau}$, where τ is the lifetime of n.[44] Then as $t\to\infty$ the δ function is replaced by a Lorentzian with width $1/\tau$. As $\tau\to\infty$ the δ function is recovered and therefore Eq. (A6) may be said to be an infinite-lifetime approximation.

Now we assume that the transition from m to n is accompanied by the absorption ($E_m < E_n$) or emission ($E_m > E_n$) of a photon and that emitted photons travel in the same direction as those described by $\vec{A}(t)$. Let the photon density be U. The rate of change of U is

$$\frac{dU}{dt} = \lim_{t \to 0} \left(\frac{U(t) - U(0)}{t} \right) , \tag{A7}$$

where

$$U(t) = U(0) - N_a(t) + N_e(t) \tag{A8}$$

and $N_a(t)$ [or $N_e(t)$] is the number of photons per unit volume absorbed (or emitted) in time t. $N_a(t)$ and $N_e(t)$ are given by

$$N(t) = \frac{\sigma}{4\pi} \int_0^{\pi} \int_0^{2\pi} \sin\theta \sum_{m,n}{}' W_{m \to n}(t) P_m \, d\theta \, d\varphi , \tag{A9}$$

where σ is the number of molecules per unit volume, P_m is the probability that a molecule is in state m at $t = 0$, and the prime on the summation indicates that the terms for which $E_m > E_n$ ($E_m < E_n$) are omitted for absorption (emission). We take P_m to be the thermal probability,

$$P_m = (1/Z) e^{-E_m/kT} , \tag{A10}$$

where

$$Z = \sum_m e^{-E_m/kT} \tag{A11}$$

is the partition function for a molecule at temperature T. Combining Eqs. (A6)–(A10) and performing the integration over the molecular orientations yields

$$\frac{dU}{dt} = \frac{\pi \sigma e^2 A_0^2 \Omega^2}{6c^2 \hbar^2 Z} \sum_m \sum_{n>0} |\langle m | r | m+n \rangle|^2 \times (e^{-E_{m+n}/kT} - e^{-E_m/kT}) \delta(\omega_{m+n} - \omega_m - \Omega) . \tag{A12}$$

The intensity of light passing through an absorbing medium as a function of distance, x, is given by the empirical relation $I = I_0 e^{-\beta x}$, where β is the absorption coefficient. As the photon density is proportional to I, and $x = ct/n_0$, where c/n_0 is the velocity of light in the medium, we have

$$\beta = - \frac{n_0}{cU} \frac{dU}{dt} . \tag{A13}$$

The external electric and magnetic fields are $\vec{E} = -(1/c)(\partial \vec{A}/\partial t)$ and $\vec{H} = \vec{\nabla} \times \vec{A}$ for nonmagnetic materials, where here $\vec{A} = \vec{A}_0 \cos(\vec{q} \cdot \vec{r} - \Omega t)$. The wave vector $\vec{q}$ is perpendicular to both $\vec{E}$ and $\vec{H}$ and has the magnitude $\Omega n_0/c$. The energy flux is given by $(c/4\pi)(\vec{E} \times \vec{H})$ which, when averaged over time, yields a photon flux of $n_0 \Omega A_0^2 / 8\pi c \hbar$, or a photon density of

$$U = n_0^2 \Omega A_0^2 / 8\pi c^2 \hbar . \tag{A14}$$

Substituting Eqs. (A12) and (A14) into Eq. (A13) yields Eq. (1) of Sec. III.

---

*Supported in part by the Defense Advanced Research Projects Agency under ARPA Order No. 2031.

†Present address: University of Alabama in Huntsville, Huntsville, Ala. 35807.

[1]J. R. Hardy and B. S. Agrawal, Appl. Phys. Lett. 22, 236 (1973).

[2](a) L. J. Sham and M. Sparks, Phys. Rev. B 9, 827 (1974); (b) M. Sparks, Xonics Inc. Technical Progress Final Report, 1972, under Contract No. DAHC 15-72-C-0129 (unpublished); (c) M. Sparks, Phys. Rev. B 10, 2581 (1974).

[3]T. C. McGill, R. W. Hellwarth, M. Mangir, and H. V. Winston, J. Phys. Chem. Solids 34, 2105 (1973).

[4](a) B. Bendow, S. C. Ying, and S. P. Yukon, Phys. Rev. B 8, 1679 (1973); (b) B. Bendow and S. C. Ying, Phys. Lett. A 42, 359 (1973); (c) B. Bendow, S. P. Yukon, and S. C. Ying, Phys. Rev. B 10, 2286 (1974).

[5]K. V. Namjoshi and S. S. Mitra, Phys. Rev. B 9, 815 (1974).

[6](a) D. L. Mills and A. A. Maradudin, Phys. Rev. B 8, 1617 (1973); (b) A. A. Maradudin and D. L. Mills, Phys. Rev. Lett. 31, 718 (1973); (c) D. L. Mills and A. A. Maradudin, Phys. Rev. B 10, 1713 (1974).

[7]H. B. Rosenstock, Phys. Rev. B 9, 1963 (1974); in Proceedings of the Third Conference on High Power Laser Window Materials, Cambridge, November 1974, edited by C. A. Pitah and B. Bendow (unpublished), p. 205.

[8]M. Sparks and L. J. Sham, Phys. Rev. Lett. 31, 714 (1974).

[9]B. Bendow, Appl. Phys. Lett. 23, 133 (1973).

[10]K. V. Namjoshi and S. S. Mitra (private communication).

[11]J. A. Harrington and M. Hass, Phys. Rev. Lett. 31, 710 (1973).

[12]M. Hass, J. W. Davisson, P. H. Klein, and L. L. Boyer, J. Appl. Phys. 45, 3959 (1974).

[13]T. F. Deutsch, J. Phys. Chem. Solids 34, 2091 (1973).

[14]T. F. Deutsch, Appl. Phys. Lett. 25, 109 (1974).

[15]J. W. Davisson, J. Mat. Sci. 9, 1701 (1974).

[16]P. M. Morse, Phys. Rev. 34, 57 (1929) (see also Ref. 7 for a review of the quantum mechanics of the Morse potential).

[17]K. Scholz, Z. Phys. 78, 751 (1932).

[18]L. Pauling and E. B. Wilson, *Introduction to Quantum Mechanics* (McGraw-Hill, New York, 1935), p. 82.

[19]W. Buhrer, Phys. Status Solidi 41, 789 (1970).

[20]G. Raunio and S. Rolandson, Phys. Rev. B 2, 2098 (1970).

[21]A. N. Basu and S. Sengupta, Phys. Rev. B 8, 2982 (1973).

[22]G. Dolling, H. G. Smith, R. M. Nicklow, P. R. Vigayaraghavan, and M. K. Wilkinson, Phys. Rev. 168, 970 (1968).

[23]A. M. Karo and J. R. Hardy, Phys. Rev. 181, 1272

(1969).
[30]J. P. Hurrell and V. J. Minkiewicz, Solid State Commun. 8, 463 (1970).
[25]M. Elcombe, J. Phys. C 5, 2702 (1972).
[26]M. M. Elcombe and A. W. Pryor, J. Phys. C 3, 492 (1970).
[27]R. P. Lowndes and D. H. Martin, Proc. R. Soc. Lond. A 308, 473 (1969).
[28]P. Denham, G. R. Field, P. L. R. Morse, and G. R. Wilkinson, Proc. R. Soc. Lond. A 317, 55 (1970).
[29]J. E. Rapp and H. D. Merchant, J. Appl. Phys. 44, 3919 (1973).
[30]K. K. Srivastava and H. D. Merchant, J. Phys. Chem. Solids 34, 2069 (1973).
[31]A. C. Bailey and B. Yates, Proc. Phys. Soc. Lond. 91, 390 (1967).
[32]D. L. Stierwalt and M. Hass (private communication).
[33]S. Califano and M. Czerny, Z. Phys. 150, 1 (1958).
[34]A. J. Barker, J. Phys. C 5, 2276 (1972).
[35]M. Klier, Z. Phys. 150, 49 (1958).
[36]T. F. McNelly and D. W. Pohl, Phys. Rev. Lett. 32, 1305 (1974).
[37]P. H. Klein, E. Claffy, and W. C. Collins, J. Electron. Mat. (to be published).
[38]D. W. Pohl and P. F. Meier, Phys. Rev. Lett. 32, 58 (1974).
[39]A. Mentzel, Z. Phys. 88, 178 (1934).
[40]W. Kaiser, W. G. Spitzer, R. H. Kaiser, and L. E. Howarth, Phys. Rev. 127, 1950 (1962).
[41]U. P. Oppenheim and A. Goldman, J. Opt. Soc. Am. 54, 127 (1964).
[42]H. Goldstein, *Classical Mechanics* (Addison-Wesley, Reading, 1965), p. 222.
[43]A. Messiah, *Quantum Mechanics* (North-Holland, Amsterdam, 1966), p. 725.
[44]V. Weisskopf and E. Wigner, Z. Phys. 63, 54 (1930). [See also W. Heitler, *Quantum Theory of Radiation* (Oxford U. P., Oxford, England, 1954), pp. 181–189].